A Synthesis, MAS NMR, Synchrotron X-ray Powder Diffraction, and Computational Study of Zeolite SSZ-23

Miguel A. Camblor* and María-José Díaz-Cabañas

Instituto de Tecnología Química, Universidad Politécnica de Valencia, Avda. Los Naranjos s/n, 46071 Valencia, Spain

Paul A. Cox

School of Pharmacy and Biomedical Sciences, University of Portsmouth, Portsmouth, PO1 2DT, United Kingdom

Ian J. Shannon, Paul A. Wright, and Russell E. Morris*

School of Chemistry, University of St. Andrews, St. Andrews KY16 9ST, United Kingdom

Received April 27, 1999. Revised Manuscript Received July 14, 1999

The zeolite SSZ-23 (STT) is the first zeolite found to contain channels bounded by seven and nine tetrahedral atom windows. A survey of the synthetic conditions needed to prepare SSZ-23 has been carried out, and the resulting materials characterized by synchrotron X-ray powder diffraction and magic-angle spinning NMR spectroscopy to obtain details of the long-range crystalline structure and short-range connectivity defects. The lattice energy minimized structure is in excellent agreement with the experimental results, and a comparison with other zeolites that have been simulated in this way is made.

Introduction

In 1987, workers at the Chevron Research and Technology Centre prepared a new aluminosilicate zeolite, which they designated SSZ-23, which has subsequently been given the International Zeolite Structure Commission three letter code of STT.[1] Catalytic studies showed this material to be a medium pore zeolite with considerable acidity. However, the difficulty in preparing large single crystals of this solid meant that its structure remained unsolved for more than a decade. The development of single-crystal diffraction techniques at synchrotron sources has enabled the use of extremely small crystals in structural studies. Using this technique the structure of as-made siliceous SSZ-23 was shown to contain two different kinds of pores, defined by seven and nine tetrahedral atoms, respectively.[2,3] This surprising result has overturned some conventional wisdom that had grown up surrounding zeolite chemistry; namely that large (i.e., more than five tetrahedral atom) odd-numbered rings do not exist in zeolites. This view of zeolite structure was based solely on the large number of structures containing 8-, 10-, and even 12-membered rings (MR) that had been characterized. There had previously been only one known aluminosilicate zeolite with a 7MR pore (MEI),[4] and none that had 9- or 11-membered rings. It should be noted, however, that there are other crystalline microporous materials that contain 9MR, but these are either zincosilicates (RUB-17, VPI-7) or beryllosilicates (lovdarite). Strictly speaking, these are not zeolites and, most importantly, their crystal chemistry is completely different to that of zeolites and silica. The presence of either Zn^{2+} or Be^{2+} generally gives rise to framework topologies much different to those known for zeolites.[5]

The synthesis of SSZ-23 is carried out in the presence of *N*,*N*,*N*-trimethyl-1-adamantammonium cation (TMAda$^+$) as a structure-directing agent (SDA). Zones and co-workers showed that this SDA is not specific to the formation of SSZ-23, but that other zeolites can also be formed in its presence.[1] It is also possible to prepare SSZ-23 using either fluoride or hydroxide mineralizing agents.

The tetrahedral framework of SSZ-23 can be thought of as being composed of two-dimensional arrays of cages, with molecular access between the cages in the planes of the arrays being restricted by 7MRs and 9MRs (Figure 1). A more detailed structural consideration shows that the smallest characteristic subunit of SSZ-23 consists of three 4-membered rings (4MRs) and four 5MRs. These are linked together, through 4- and 6-membered rings, to form slightly puckered layers parallel to the (101) face of the unit cell. These layers are then linked together by 4-membered rings to give the three-dimensional structure. This "pillaring" of

* Corresponding authors: rem1@st-and.ac.uk or macamblo@itq.upv.es.

(1) (a) Zones, S. I.; van Nordstrand, R. A.; Santilli, D. S.; Wilson, D. M.; Yuen, L.; Scampavia, L. D. In *Zeolites: Facts, Figures, Future*; Jacobs, P. A., van Santen, R. A., Eds.; Elsevier: Amsterdam, 1989; pp 299−309. (b) Zones, S. I. Eur. Pat. Appl. 231018, 1987.

(2) Camblor, M. A.; Díaz-Cabañas, M. J.; Perez-Pariente, J.; Teat, S. J.; Clegg, W.; Shannon, I. J.; Lightfoot, P.; Wright, P. A.; Morris, R. E. *Angew. Chem., Int. Ed. Engl.* **1998**, *37*, 2122.

(3) A 7-membered ring, 7MR (for example) is used to describe a ring in the structure that contains seven tetrahedral atoms such as silicon or aluminium and seven bridging oxygen atoms.

(4) Meier, W. M.; Olson D. H.; Baerlocher, C. *Atlas of Zeolite Structure Types*; Elsevier: New York, 1996.

(5) Camblor, M. A.; Davis, M. E. *J. Phys. Chem.* **1994**, *98*, 13151.

10.1021/cm991057r CCC: $18.00
Published on Web 09/11/1999

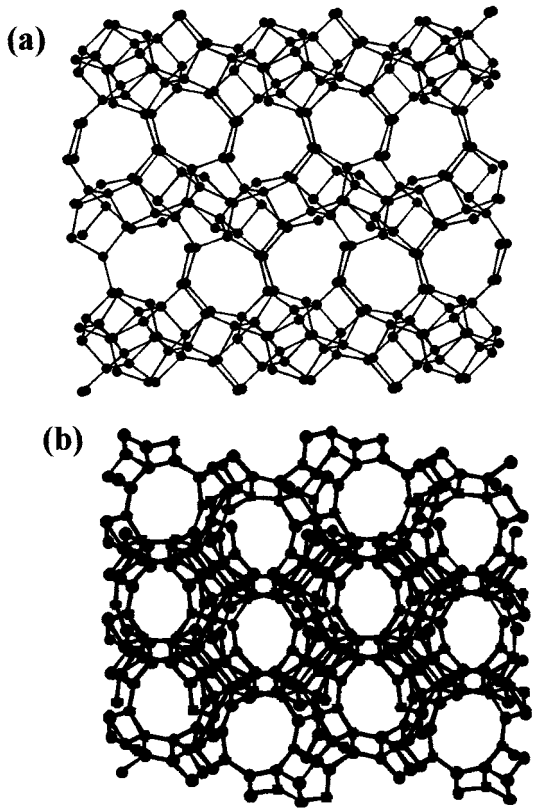

Figure 1. The structure of SSZ-23 viewed (a) parallel to the [001] direction and (b) parallel to the [101] direction. For clarity only the silicon atoms are shown. Oxygen atoms are located near the centers of the lines joining the silicon atoms.

layers produces channels running parallel to the [001] direction (Figure 1a) that are bounded at their narrowest points by 7MR windows. Parallel to the [101] direction are the channels bounded by 9MR windows, slightly offset from one to the next (Figure 1b). Cages are located at the intersection of the 7- and 9MR channels, inside which the *N*,*N*,*N*-trimethyl-1-adamantammonium cation ($TMAda^+$) structure-directing agent is located. Zeolite SSZ-23 was also found to have some other unusual structural features. Noteworthy among these was the presence of SiO_4F units in the structure (i.e., five-coordinated silicon). Subsequently, further NMR studies have demonstrated that the SiO_4F unit is far more common in zeolites prepared in F^- media than was once believed.[6,7] The ^{29}Si MAS NMR results (see below) suggest at room-temperature F^--to- Si bonds in SSZ-23 reorient very fast. Reference 7 shows by a number of NMR techniques that when SSZ-23 is cooled F^- jumping is frozen and at 140 K the pentacoordinate units are completely localized. On calcination, however, the fluoride ions were lost from the structure and the zeolite reverts to being wholly tetrahedral.

The discovery that SSZ-23 contains large pores defined by 7- and 9MR opens up the possibility of using this strongly acidic zeolite as a shape-selective catalyst. Previous experiments have shown that the adsorption properties of SSZ-23 differ considerably from those of 8- and 10MR containing zeolites. For example, *n*-hexane is adsorbed much more readily than 3-methylpentane and 2,2-dimethylbutane. This is in strong contrast to ZSM-5. In addition to the potential uses of SSZ-23, the discovery of 9MR and five-coordinate silicon poses some interesting and fundamental questions relating to the synthesis and structure of zeolites. Foremost among these is why there are so many 8- and 10MR structures known but only one 9MR zeolite so far. Is there something intrinsically unfavorable about large odd-membered ring systems? Furthermore, SSZ-23 is just one zeolite product prepared using the $TMAda^+$ cation as a template, and a careful study is required to disentangle the multiple influences of time, reagents and gel dilution on the synthesis. In this paper we report the results of a survey of the synthesis of SSZ-23 and the characterization of SSZ-23 using MAS NMR and synchrotron powder X-ray diffraction. A computational study of the lattice energy and the location of template molecules in the cages is also reported.

Experimental Section

1. Synthesis. All the syntheses involved the use of *N*,*N*,*N*-trimethyl-1-adamantammonium cation ($TMAda^+$) in hydroxide form as an organic structure-directing agent (SDA). The $TMAda^+$ was prepared by quaternization of the parent primary amine. In a typical synthesis 1-adamantamine (4.667 g) was dissolved in 50 g of chloroform. Then, 11.350 g of $K_2CO_3 \cdot 1.5H_2O$ was added, and the mixture was cooled in an ice bath. A total of 13.14 g of CH_3I was then added, followed the next day by a second portion of CH_3I (6.5 g). After 7 days, the mixture was filtered, and the solid was washed with $CHCl_3$. The $CHCl_3$ solution was then rotovaporated under vacuum to obtain the trimethyladamantammonium iodide as a white powder. The iodide was converted to the hydroxide by anion exchange with Dowex 1 resin.

For the zeolite synthesis, hydrothermal crystallization was attempted using either hydroxide or fluoride anions as mineralizers. For fluoride syntheses the effect of the degree of dilution of the reaction mixture on the phase selectivity of the crystallization was investigated. Unless otherwise noted, the reaction mixture composition for the synthesis using fluoride was SiO_2:0.50 TMAdaOH:0.50 HF:*x* H_2O and the final water-to-silica ratio (*x* in the above composition) was varied between 3 and 20. Tetraethyl orthosilicate (TEOS) was used as a silica source (unless otherwise noted) and the ethanol produced after its hydrolysis was completely evaporated.

In a typical synthesis yielding pure silica SSZ-23, 15.60 g of tetraethyl orthosilicate was hydrolyzed in 86.10 g of a 0.435 M solution of TMAdaOH, and the mixture was stirred until all of the ethanol produced had evaporated and a final H_2O/SiO_2 ratio of 10 attained. Then 1.56 g of HF (aqueous, 48%) was added, the viscous gel was then stirred thoroughly by hand, and the mixture was transferred to Teflon-lined stainless steel autoclaves and heated at 150 °C for 15 days while being rotated at 60 rpm. Afterward, the autoclave was quenched and the contents (pH = 7.9) were filtered, washed, and dried at 100 °C. The yield of solids was 20.35 wt % (around 98% based on SiO_2).

2. Phase and Composition Characterization. Phase purity and crystallinity were determined by conventional powder X-ray diffraction (XRD) using a Philips X'Pert diffractometer (Cu Kα radiation, graphite monochromator) equipped with a variable divergence slit and a proportional Xe detector and working in the fixed irradiated area mode. C, H, and N contents were determined with a Carlo Erba 1106 elemental organic analyzer. Fluoride content was determined using an ion-selective electrode connected to a Mettler Toledo 355 ion analyzer after dissolution of the as-made solids by a standard procedure.[8]

3. Magic-Angle Spinning NMR. ^{29}Si and ^1H MAS NMR and ^{13}C CPMAS NMR spectra of the solids were recorded on

(6) Koller, H.; Wölker, A.; Eckert, H.; Panz, Ch.; Behrens, P. *Angew. Chem., Int. Ed. Engl.* **1997**, *36*, 2823−2825.
(7) Koller, H.; Wölker, A., Villescusa, L. A.; Díaz-Cabañas, M. J.; Valencia, S.; Camblor, M. A. *J. Am. Chem. Soc.* **1999**, *121*, 3368.

a Varian VXR 400SWB spectrometer. The ^{29}Si MAS NMR spectra were recorded with a spinning rate of 5.5 kHz at a ^{29}Si frequency of 79.459 MHz with a 55.4° pulse length of 4.0 μs and a recycle delay of 240 and 60 s for the as-made and calcined samples, respectively. The ^{1}H MAS NMR spectra were recorded with a spinning rate of 7.0 kHz at a ^{1}H frequency of 399.956 MHz with a pulse length of 1.0 μs and a recycle delay of 5.0 s. The ^{13}C CPMAS NMR spectra were acquired with a spinning rate of 5 kHz at a ^{13}C frequency of 100.579 MHz with a 70° pulse length of 5.5 μs, a contact time of 5000 μs and a recycle delay of 3 s. The ^{1}H, ^{29}Si, and ^{13}C chemical shifts are reported relative to TMS.

4. Synchrotron X-ray Powder Diffraction. Room-temperature synchrotron X-ray powder diffraction data were collected on beamline BM16 at the European Synchrotron Radiation Facility in Grenoble, France. The experiment used a wavelength of 0.6005 Å, selected using a sagitally focusing Si(111) double-crystal monochromator. Data were collected on a calcined (i.e., template free) sample of SSZ-23 over an angular range of $1° > 2\theta > 20°$. Rietveld analysis of the data was accomplished using the GSAS suite of programs[9] using the silicon and oxygen atomic positions from the previously accomplished microcrystal X-ray diffraction study of templated SSZ-23 as a starting model.

5. Computer Simulation Experiments. The program GULP (General Utility Lattice Program), which was developed by Gale,[10] was used to perform symmetry-adapted, lattice energy minimizations of the SSZ-23 structure. All minimizations were carried out at constant pressure and used the empirical force field for silicates developed by Sanders et al.[11] The calculations were carried out on a Silicon Graphics machine with 128 MB of memory.

The location of the template molecule inside the framework was determined using a Monte Carlo−simulated annealing (MC−SA) method.[12] The geometry of the template molecule was optimized outside the framework energy minimization methods. The maximum number of templates (four) were then docked into the unit cell of the SSZ-23 framework using the Monte Carlo method with an energy threshold of 1000 kcal mol^{-1}. The location/conformation of the template molecules were then optimized using a simulated annealing routine that ran for 500 cycles with at time step of 1×10^{-15} s at temperatures of 1000, 750, 500, 300, 200, and 100 K, followed by a final energy minimization. Periodic boundary conditions and a rigid, fully siliceous lattice were used for the MC−SA calculation. The modified CVFF force field within the program Discover 3.1 was used throughout.[13] All results reported represent the lowest energy configuration from 25 independent MC−SA runs.

Results and Discussion

1. Synthesis from Fluoride Media. Table 1 summarizes the results of the synthesis of pure silica phases using TMAda$^+$ as a structure-directing agent. The table shows that by just varying the degree of dilution of the synthesis mixture using fluoride as a mineralizer, three different zeolitic phases may be obtained: chabazite (CHA, comprising a three-dimensional system of 8-member ring channels, 3D 8MR), SSZ-23 (STT, 2D 7MR+9MR), and SSZ-31 (1D, 12MR). Much has been written and discussed about structure direction effects in the synthesis of zeolites.[14] However, the degree of dilution of the synthesis mixture, characterized by the water-to-silica ratio (or the concentration of the SDA, see below) has not been considered as a critical factor in determining the phase selectivity during the crystallization of zeolites until very recently.[15−17] During the course of a systematic investigation on the synthesis of high and pure silica zeolites in fluoride aqueous media, we noticed that, generally, the phase selectivity of the crystallization is highly dependent on the degree of dilution of the reacting mixture.[16] Keeping other parameters constant, a given SDA frequently produces different silica structures at different H_2O/SiO_2 ratios. Moreover, the usual trend is that the higher the H_2O/SiO_2 ratio in the synthesis mixture the higher the framework density of the silica phase formed (although we recently found one exception to this trend).[17] This appears to be the case when the SDA is the trimethyladamantammonium cation (TMAda$^+$), as shown in Table 1. For pure silica compositions, as the water/silica ratio increases the first crystallization product changes from pure silica chabazite (CHA, framework density (FD): 15.4Si/1000 Å^3) to SSZ-23 (STT, FD: 17.0), and SSZ-31 (FD: 18.7). However, it is interesting that SSZ-23 is the final phase found for any water content under

Table 1. Synthesis Conditions and Results[a]

H_2O/SiO_2	*t* (days)	phase
44[b,c]	15	unknown layered phase + SSZ-23
	18	SSZ-23
	21	SSZ-23
44[d]	15	amorphous
	22	tridymite
20	6	SSZ-31 + amorphous
	9	SSZ-31 + SSZ-23
	12	SSZ-23
15	10	SSZ-31 + amorphous (+ minor SSZ-23)
	25	SSZ-23 + SSZ-31
	30	SSZ-23
15[c]	7	amorphous
	14	amorphous + SSZ-23
	21	SSZ-23
10	6	SSZ-23 + amorphous
	11	SSZ-23
7.5	7	SSZ-23
5.8	3	SSZ-23 + CHA + amorphous
	5	SSZ-23 + CHA
	7	SSZ-23 (+ minor CHA)
3	0.6	unknown layered phase + CHA + amorphous
	1	CHA + unknown layered phase
	1.6	CHA
	7	CHA + SSZ-23

[a] For crystallizations at 150 °C under slow rotation (60 rpm) using a reaction composition of SiO_2:0.50 TMAdaOH:0.50 HF:*x* H_2O, unless otherwise noted. The H_2O/SiO_2 ratio is given by *x* in the above formula. [b] Chemical composition: SiO_2:0.25 TMAdaOH:44 H_2O. [c] Ludox AS-40 used as a source of silica. In all the other experiments TEOS was used (see text for experimental details). [d] Chemical composition: SiO_2:0.25 TMAdaOH:0.25 HF:44 H_2O.

(8) Guth, J. L.; Wey, R. *Bull. Soc. Fr. Minéral. Cristallogr.* **1969**, *92*, 105.
(9) Larson, A. C.; Von Dreele, R. B. Los Alamos Laboratory Report, 1987, No LA-UR-86−748.
(10) GULP (the General Utility Lattice Program) written and developed by J. D. Gale; Royal Institution/Imperial College: United Kingdom, 1992−1994.
(11) Sanders, M. J.; Leslie, M.; Catlow, C. R. A. *J. Chem. Soc., Chem. Commun.* **1984**, 1271.
(12) Stevens, A. P.; Gorman A. M.; Freeman, C. M.; Cox, P. A. *J. Chem. Soc., Faraday Trans.* **1996**, *92*, 2065.
(13) Discover 3.1 program; MSI: San Diego, CA, 1993.
(14) Lobo, R. F.; Zones, S. I.; Davis, M. E. *J. Inclusion Phenom. Mol. Recogn. Chem.* **1995**, *21*, 47.
(15) Gies, H.; Marler, B.; Werthman, S. In *Molecular Sieves: Science and Technology*; Karge, H. G., Weitkamp, J., Eds.; Springer: Berlin, 1998; p 35.
(16) Barrett, P. A.; Boix, E. T.; Camblor, M. A.; Corma, A.; Díaz-Cabañas, M. J.; Valencia, S.; Villaescusa, L. A. In *Proceedings of the 12th International Zeolite Conference*, Treacy, M. M. J., Marcus, B. K., Bisher, M. E., Higgins, J. B., Eds.; Materials Research Society: Warrendale, PA, 1999; p 1495.
(17) Camblor, M. A.; Villaescusa, L. A.; Díaz-Cabañas, M. J. *Top. Catal.*, in press.

Table 2. Chemical Composition of As-Made SSZ-23 Silica Samples

	g/100 g of solid				molar ratios		
mineralizer	N	C	H	F	C/N	H/N	F/N
F^-	1.20	13.50	2.16	1.32	13.1	25.0	0.81
OH^-	1.25	13.30	2.34		12.4	26.0	

the reported conditions and crystallization times. Thus, at low water contents fully crystallized CHA appears to be metastable and experiences an Ostwald ripening transformation to SSZ-23, which is thus concluded to be a more stable phase in this synthesis medium. In the high water content region, SSZ-23 nucleates and grows before full crystallization of SSZ-31, and thus the phenomenon is not a true Ostwald ripening but a cocrystallization process, and no definitive conclusion on their relative stabilities can be drawn.

It is worth to noting that in the synthesis of silica phases in hydroxide media using neutral amines as SDA's Gies and co-workers have observed a trend similar to ours:[15] as the concentration of the SDA (or SDA/SiO_2 ratio) increases the density of cages in the phase obtained increases. In our case, using a cationic SDA in fluoride media the same trend is observed: as the H_2O/SiO_2 ratio decreases (i.e., SDA concentration increases) the cage density increases from 0 (SSZ-31) to 1.06 (SSZ-23) and 1.28 cages/1000 Å^3 (CHA). However, it must be taken into account that changing the water content of the synthesis mixture would not only affect the SDA concentration but also the F concentration. Given that F is finally occluded in the zeolite and that it may have an structure-directing effect[15] this may have an effect in the phase selectivity in addition to that of the SDA concentration and should not be neglected. Additionally, we have shown that our observed trend on FD holds also for cases in which there are no obvious cages, as in the synthesis of CFI and AFI using methylsparteinium as SDA in fluoride medium.[18] From this point of view, while there is usually a correspondence between cage density and framework density, it appears preferable to express the trend in terms of framework density.

$TMAda^+$ is a structure-directing cation of rather low specificity as it can direct the crystallization of many different silica-based microporous phases (AFI, STT, CHA, VET, MWW, etc.). However, this cation appears to show some preference toward SSZ-23 when the synthesis is carried out in fluoride medium, giving a rather broad synthesis window in these conditions.

When synthesized from fluoride aqueous media, SSZ-23 occludes almost equivalent amounts of $TMAda^+$ and fluoride ions (Table 2). The integrity of the organic cation occluded in SSZ-23 can be safely ascertained by means of the chemical composition (C/N ratio very close to the expected value of 13) and ^{13}C CPMAS NMR experiments (Figure 2). A small misbalance between $TMAda^+$ and F^- ions in the sample prepared in fluoride medium (Table 2) suggests the presence of a small but nonnegligible concentration of connectivity defects in the SiO_2 framework (around 0.7−0.8 charged Si−O^- defects per unit cell). The presence of defects was confirmed by ^{29}Si MAS NMR spectroscopy of the as-made sample

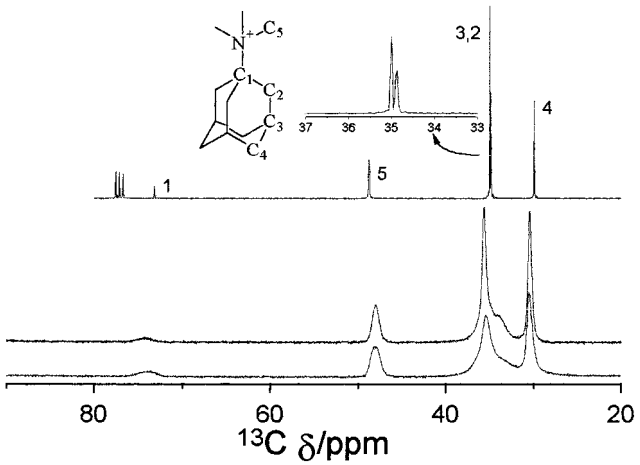

Figure 2. ^{13}C CPMAS NMR spectra of as-made SSZ-23 prepared in hydroxide (bottom) and fluoride media (middle) and ^{13}C NMR spectrum of trimethyladamantammonium iodide dissolved in $CDCl_3$ (top and insert; the figures near each peak are the assignments to the corresponding C in the drawing).

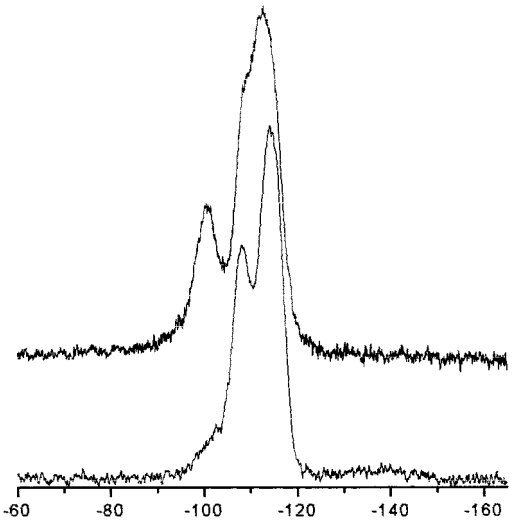

Figure 3. ^{29}Si MAS NMR spectra of as-made SSZ-23 prepared in hydroxide (top) and fluoride media (bottom).

(Figure 3), which reveals around 2.7% of the Si atoms are Q^3 species. This represents around 1.7 defects per unit cell, i.e., twice the amount of required charged defects, suggesting that connectivity defects appear as couples of Si−O^- and Si−OH groups. ^1H MAS NMR spectroscopy of the as-made solid (Figure 4) further confirms the presence of charged Si−O^- and Si−OH groups. As shown in Figure 4, there is a small band at around 9.9 ppm that may be assigned to protons involved in Si−OH···$^-$O−Si hydrogen-bonded groups.[19] No such band appears in the spectrum of the calcined samples. Taking into account the composition shown in Table 2 and the relative intensity of this band with respect to the total intensity of the spectrum, we have estimated the relative amount of protons in Si−O^-··· HO−Si groups in SSZ-23 as 0.2 H per N (or 0.8 H per unit cell). This is in good agreement with the expected amount of Si−O^- groups, suggesting that each Si−O^- group is involved in just one hydrogen bond to a nearby HO−Si group.

(18) Barrett, P. A.; Diaz-Cabanas, M. J.; Camblor, M. A.; Jones, R. H. *J. Chem. Soc., Faraday Trans.* **1998**, *94*, 2475.

(19) Koller, H.; Lobo, R. F.; Burkett, S. L.; Davis, M. E. *J. Phys. Chem.* **1995**, *99*, 12588.

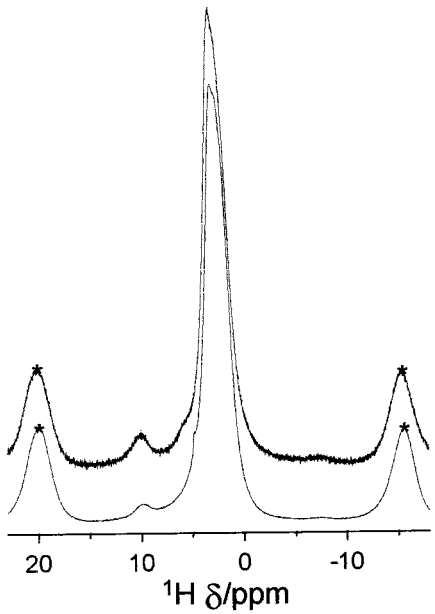

Figure 4. ^{1}H MAS NMR spectra of as-made SSZ-23 prepared in hydroxide (top) and fluoride media (bottom).

2. Synthesis from Hydroxide Media. Pure silica SSZ-23 can also be synthesized in hydroxide medium using $TMAda^+$ as SDA (Table 1, first entry), although in this case we have used a much more diluted reaction mixture, due to the relatively low stability of the $TMAda^+$ cation in a highly alkaline hydrothermal medium. No SSZ-31 was found under these conditions. When HF was added to this reaction mixture in equimolar amounts to TMAdaOH, the only crystalline phase obtained was tridymite.

When the synthesis is carried out in hydroxide medium we observed a decreased C/N ratio in the elemental analysis which could be due to significant degradation of the SDA although the ^{13}C CP MAS NMR spectrum (Figure 2) also shows the expected resonances (broader than in the fluoride sample).

The lack of fluoride ions in the hydroxide-prepared solid means that there must be a larger concentration of $Si-O^-$ defect groups than in the fluoride-prepared solid to achieve full charge balance. The ^{29}Si MAS NMR spectrum (Figure 3) shows the presence of a very prominent band at −100.6 ppm assigned to Q^3 defect sites and amounting to 25% of the Si atoms (16 Si per unit cell). Thus, the concentration of defects exceeds in this case the concentration of charged cations by a factor of 4, as usually found in pure and very high silica zeolites prepared in hydroxide medium.[19,20] ^{1}H MAS NMR spectroscopy of the as-made solid (Figure 4) shows the presence of a band around 10.0 ppm with a larger relative intensity than the 9.9 ppm band of the fluoride sample. The concentration of protons in $Si-O^-\cdots HO-Si$ groups in the OH^- sample has been estimated as 0.55 H per N (or 2.2 per unit cell). Resonances due to other types of Si−OH groups, not involved in hydrogen bonds to $Si-O^-$, are also present in the ^{1}H MAS NMR spectra of both SSZ-23 samples: one broad band at 5.8 ppm in both samples (more evident in the sample prepared in OH^- medium) and a very small and sharp band at 4.7 ppm in the sample prepared in F^- medium may be assigned to Si−OH groups forming relatively weak hydrogen bonds, possibly including silanols in the outer surface of the crystallites.[21] The band at 4.7 ppm could also be due to small water clusters or to moisture in the outer surface of the crystallites,[21] by comparison with the chemical shift of liquid water (4.8 ppm). Still more bands could also be present in the 6−0 ppm range, in which the intense and broad resonances coming from the organic matter dominate (3.3, 2.4, 2.1, and 1.7 ppm for $TMAda^+$).

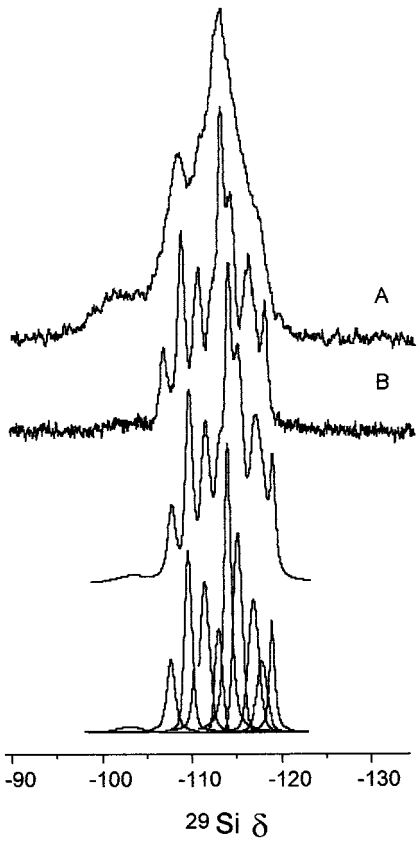

Figure 5. ^{29}Si MAS NMR spectra of calcined SSZ-23 prepared in hydroxide (A) and fluoride media (B). The lower traces correspond to the deconvolution of spectrum B.

3. Calcined Samples. The guest species occluded in SSZ-23 may be removed by calcination at 580 °C for 3 h. In the samples prepared in fluoride media the occluded fluoride anion was determined to be located inside a small $[4^35^4]$ cage within the SiO_2 framework by single-crystal microcrystal diffraction.[2] A broad band in the −130 to −150 ppm range of the ^{29}Si MAS NMR spectrum of the as-made solid (Figure 3) was assigned to five-coordinated $[SiO_{4/2}F]^-$ species in which F^- jumps between several Si sites.[2,7] After calcination this band disappears (Figure 5), confirming the removal of fluoride, and only resonances in the range corresponding to $Si(OSi)_4$ species are clearly detected. However, there is a broad, very small and hardly detectable band near −102 ppm which must be assigned to a very small concentration (<1.5%) of connectivity defects. This suggests about a half of the defects detected in the as-made solid (2.7% according to the ^{29}Si MAS NMR

(20) Camblor, M. A.; Corma, A.; Valencia, S. *Microporous Mesoporous Mater.* **1998**, *25*, 59.

(21) Villaescusa, L. A.; Barrett, P. A.; Camblor, M. A. *Chem. Mater.* **1998**, *10*, 3966.

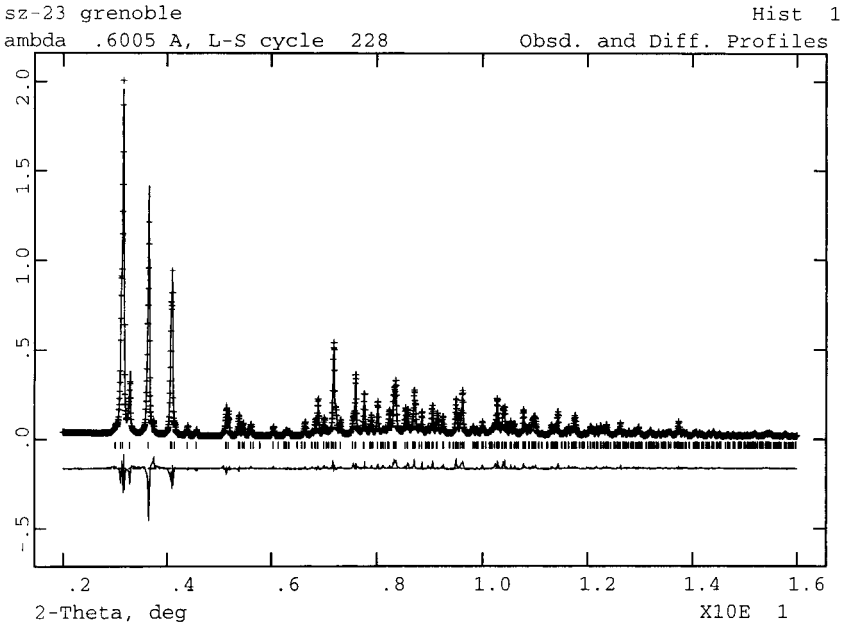

Figure 6. Final observed, calculated, and difference plots for the Rietveld refinement of calcined SSZ-23 against synchrotron X-ray powder diffraction data.

spectrum of the as-made solid) are annealed upon calcination. For the sample prepared in OH^- medium, the concentration of Si−OH defects found in the ^{29}Si MAS NMR spectrum after calcination (Figure 5, around 15% of the Si) is also reduced with respect to that found in the as-made material (25%).

The ^{29}Si MAS NMR spectra show large differences between the calcined silica samples prepared in hydroxide and fluoride media (Figure 5). In addition to the different intensity of the band at around −100 ppm commented above, the region of $Si(OSi)_4$ species is very nicely resolved in the sample prepared in fluoride medium, while it shows a very poor resolution in the sample prepared in hydroxide medium. This is attributed to the presence of a large concentration of defects in the latter sample. If these defects are randomly distributed this will affect the short-range order of the material, producing broad and ill-defined bands. The experimental observation that silica zeolites prepared in hydroxide media show a very large concentration of connectivity defects while those prepared in fluoride media show a very small (if any) concentration of such defects is discussed and rationalized elsewhere.[17] This is as a consequence of several factors: the nature of the main negative species affording charge balance of the organic cation ($Si-O^-$ or F^-), stabilization of additional Si−OH groups by $Si-OH\cdots{}^-O-Si$ hydrogen bonds, different pH of the reacting mixture, and possibly, annealing of defects catalyzed by HF produced during the calcination of the materials prepared in fluoride media. Thus, the very small concentration of defects in the sample prepared in fluoride medium allows a high resolution of $Si(OSi)_4$ species in different crystallographic sites. Up to nine $Si(OSi)_4$ resonances from −107.1 to −118.4 ppm are clearly detected (Figure 5), suggesting that the average Si−O−Si angle for every Si site is in the 141−160.5° range (calculated by applying the equation of Thomas et al.).[22] This is in reasonable agreement with the average angles found by Rietveld refinement (see below) which are in the range 143.7−161.6°. A deconvolution of the spectrum of the sample prepared in fluoride medium consisting of nine $Si(OSi)_4$ components with approximate relative intensities of 1:2:2:1:3:3:2:1:1 is also shown in Figure 5. This is consistent with the structure proposed below, in which Si is in 16 different crystallographic sites with equal multiplicity.

4. Powder Diffraction Study. Rietveld refinement of the structural model for SSZ-23 (fluoride preparation, calcined at 500 °C in flowing oxygen) against synchrotron X-ray diffraction data was completed using the GSAS suite of programs. The rather complex nature of the SSZ-23 structure, with 16 crystallographically independent silicon sites meant that soft constraints on the Si−O bond distances (1.6 Å) were necessary to ensure that the refinement was stable. The final cycle of least-squares refinement included terms for the unit cell constants, atomic positions of Si and O, and one isotropic temperature factor for silicon and one for oxygen. The peak shape function was pseudo-Voigt, corrected for peak asymmetry using the function of Finger et al.[23] The refinement converged to final agreement values of Rwp = 0.0935, Rp = 0.0772, and R_F^2 = 0.0789. The final refined unit cell was a = 13.0916 (4) Å, b = 21.7078 (6) Å, c = 13.7084(3) Å, and β = 102.534 (3)°. The final observed, calculated, and difference plots from the Rietveld refinement are shown in Figure 6. The refined model confirms that the framework structure of SSZ-23 remains intact on calcination. The average Si−O−Si bond angles for each silicon are in the range 143.7−161.6°, which correlates well with those calculated from the ^{29}Si MAS NMR shifts (see above).

5. Computer Simulations. The calculated lattice parameters and fractional coordinates of SSZ-23 show excellent agreement with the experimentally deter-

(22) Thomas, J. M.; Klinowski, J.; Ramdas, S.; Hunter, B. K.; Tennakoon, D. T. B. *Chem. Phys. Lett.* **1983**, *102*, 158.
(23) Finger, L. W.; Cox, D. E.; Jephcoat, A. P. *J. Appl. Crystallogr.* **1994**, *27*, 892.

Table 3. Final Atomic Coordinates (ESDs in parentheses) from the Experimental Structure Determination and from the Calculation

atom	*x*(exp)	*y*(exp)	*z*(exp)	*x*(calcd)	*y*(calcd)	*z*(calcd)
Si1	0.5959 (17)	0.1681 (10)	0.2005 (16)	0.59097	0.16607	0.20431
Si2	0.6259 (18)	0.1670 (9)	0.4333 (16)	0.63381	0.16749	0.43849
Si3	0.6966 (19)	0.5709 (9)	−0.0361 (17)	0.69946	0.57167	−0.03922
Si4	0.6614 (18)	0.4925 (10)	0.1342 (16)	0.66601	0.49376	0.13353
Si5	0.6698 (17)	0.3008 (11)	0.2187 (16)	0.66286	0.30136	0.21847
Si6	0.6855 (16)	0.3043 (10)	0.4539 (14)	0.68780	0.30635	0.44714
Si7	0.4987 (19)	0.4037 (10)	0.1961 (16)	0.50238	0.40614	0.19495
Si8	0.4588 (18)	0.1027 (9)	0.5156 (17)	0.46538	0.09743	0.52002
Si9	0.7728 (17)	0.5524 (10)	0.3378 (16)	0.77382	0.55260	0.33186
Si10	0.3688 (15)	−0.0020 (10)	0.3768 (15)	0.37232	−0.00164	0.37677
Si11	0.1461 (16)	0.4982 (10)	0.3546 (15)	0.14701	0.50064	0.35443
Si12	0.8234 (18)	0.3830 (10)	0.1675 (16)	0.82566	0.38523	0.16425
Si13	0.5299 (19)	0.4156 (10)	0.4336 (15)	0.53400	0.41512	0.42734
Si14	0.8927 (18)	0.3720 (9)	0.5572 (17)	0.88908	0.37277	0.55713
Si15	0.3477 (18)	0.4573 (11)	0.5064 (16)	0.34449	0.46183	0.50392
Si16	0.9336 (16)	0.4384 (10)	0.3739 (17)	0.93021	0.43991	0.36998
O1	0.6359 (24)	0.5349 (15)	0.0370 (21)	0.64063	0.53171	0.03093
O2	0.5868 (28)	0.1583 (15)	0.3141 (16)	0.59108	0.15894	0.32058
O3	0.9000 (25)	0.3995 (14)	0.2737 (19)	0.89893	0.39778	0.27228
O4	0.6551 (27)	0.2350 (11)	0.4760 (23)	0.65931	0.23734	0.47164
O5	0.5338 (22)	0.1558 (13)	0.4902 (26)	0.54338	0.14754	0.49314
O6	0.7580 (28)	0.3196 (14)	0.1546 (30)	0.75213	0.32639	0.16576
O7	0.7527 (26)	0.4432 (14)	0.1264 (25)	0.75745	0.44563	0.12869
O8	0.6496 (27)	0.2312 (11)	0.1801 (26)	0.64143	0.23115	0.18545
O9	0.4306 (25)	0.4083 (14)	0.4827 (28)	0.43294	0.41804	0.47592
O10	0.9448 (23)	0.3941 (15)	0.4670 (20)	0.93796	0.39646	0.46572
O11	0.3964 (28)	0.1309 (15)	0.5914 (24)	0.39297	0.13142	0.58357
O12	0.5578 (24)	0.4587 (14)	0.1513 (25)	0.56288	0.46064	0.15185
O29	0.6198 (21)	0.5963 (14)	−0.1354 (22)	0.61431	0.59959	−0.12993
O14	0.7308 (21)	0.1260 (14)	0.4743 (25)	0.73707	0.12662	0.47480
O15	0.5019 (26)	0.4169 (16)	0.3136 (16)	0.49880	0.42182	0.30823
O16	0.3873 (26)	0.0659 (12)	0.4236 (23)	0.39685	0.06724	0.41968
O17	0.7097 (28)	0.5364 (15)	0.2272 (18)	0.70735	0.54193	0.22144
O18	0.6663 (28)	0.1147 (13)	0.1701 (26)	0.65438	0.11172	0.16693
O19	0.4783 (20)	0.1620 (16)	0.1408 (22)	0.47397	0.16353	0.13885
O20	0.5940 (26)	0.3531 (13)	0.4579 (25)	0.59235	0.35068	0.45842
O21	0.5313 (23)	0.0472 (13)	0.5775 (24)	0.52505	0.04318	0.58922
O22	0.2522 (21)	0.4684 (16)	0.4134 (22)	0.24582	0.46209	0.41168
O23	0.7668 (22)	0.5236 (15)	−0.0862 (25)	0.77565	0.52801	−0.08365
O24	0.6976 (28)	0.5713 (16)	0.4066 (23)	0.69259	0.56626	0.40141
O25	0.1464 (27)	0.5675 (12)	0.3917 (24)	0.15527	0.57042	0.39124
O26	0.7007 (26)	0.3069 (17)	0.3397 (16)	0.70648	0.31005	0.33593
O27	0.5648 (24)	0.3417 (13)	0.1818 (25)	0.55711	0.34083	0.18584
O28	0.8553 (24)	0.4963 (12)	0.3703 (24)	0.84370	0.49268	0.37233
O29	0.0425 (20)	0.4616 (16)	0.3573 (26)	0.04142	0.47079	0.37371
O30	0.3483 (30)	0.0031 (15)	0.2582 (16)	0.34582	0.00092	0.25915
O31	0.7936 (19)	0.3264 (15)	0.5245 (22)	0.79469	0.32551	0.52096
O32	0.6065 (26)	0.4735 (13)	0.4684 (24)	0.61362	0.46937	0.47041

mined values (see Table 3). The calculated cell parameters a(calcd) = 13.0899 Å, b(calcd) = 21.6701 Å, c(calcd) = 13.7347 Å, and β(calcd) = 102.578° are all comfortably within 1% of the experimentally observed values, as are the calculated and experimentally observed cell volumes. This is remarkable considering the relatively large volume of the cell and crystallographic complexity of the structure.

The value of the total calculated lattice energy for SSZ-23, 13.85 kJ mol^{-1} (relative to quartz), compares very well with the values for other siliceous zeolites that have been calculated using similar methods by Henson, Cheetham, and Gale.[24] All the siliceous zeolites so far studied have calculated lattice energies between 5 and 20 kJ mol^{-1} greater than that of quartz. Furthermore, the siliceous zeolites studied by these researchers showed a marked correlation between calculated energy and framework density. SSZ-23 is of fairly low density at around 17 tetrahedral atoms per 1000 Å^3, which is intermediate between that of zeolites ferrierite (FER) and beta (BEA). SSZ-23 fits extremely well onto the correlation of lattice energy with framework density (see Figure 7). The fact that the calculated lattice energy for SSZ-23 maps onto this correlation so well strongly suggests that there is nothing intrinsically unstable (e.g., no ring strain), at least when compared to other zeolite frameworks, of a structure containing large odd-numbered ring windows. The relative paucity of 7- and 9-membered ring zeolites must therefore be due to other reasons.

As described above, the TMAda$^+$ templating agent is not very specific for SSZ-23, especially in fluoride-free syntheses. However, the microcrystal X-ray diffraction study did reveal that the template was well-ordered and located inside a small cavity, which is formed at the intersection of the 7MR and 9MR channels. Docking calculations were then carried out to evaluate whether this template position could be reproduced in a computer simulation. The results (Figure 8) show the excellent

(24) Henson, N. J.; Cheetham, A. K.; Gale, J. D. *Chem. Mater.* **1994**, *6*, 1647.

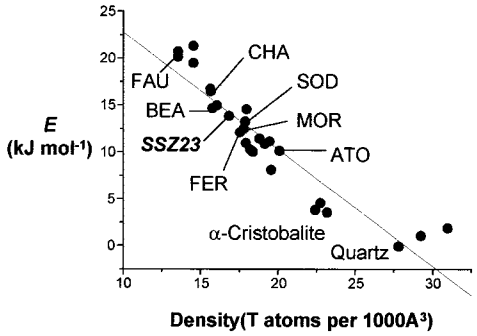

Figure 7. Variation of calculated lattice energy with density for silica structures, showing that SSZ-23 fits onto the same correlation as the other structures. For clarity, only some of the silica structures are labeled. The data for the other zeolite structures was taken from ref 24.

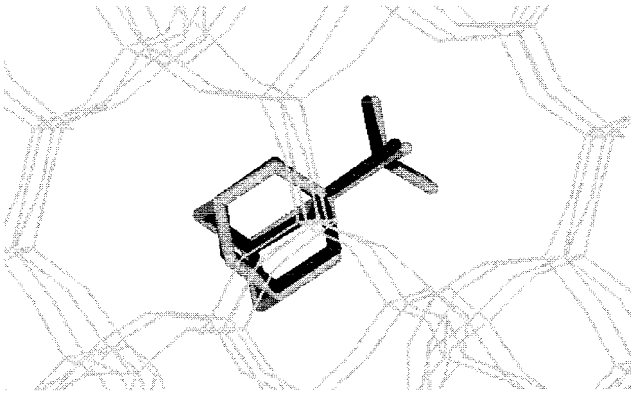

Figure 8. Comparison of the experimental (black) and calculated (grey) positions for the *N*,*N*,*N*-trimethyl-1-adamantammonium cation in SSZ-23.

agreement between these calculations and the experimentally observed template positions taken from ref 2.

Conclusions

The degree of dilution of the reaction mixture may be a critical parameter in determining the phase selectivity during the crystallization of pure silica zeolites in the presence of fluoride anions as mineralizers and organic cations as structure-directing agents. This has been shown here for the case of trimethyladamantammonium, since with this SDA cation three different zeolites (SSZ-23, CHA, and SSZ-31) may crystallize by just varying the H_2O/SiO_2 ratio of the synthesis mixture. However, under the reported synthesis conditions SSZ-23 appears to be the most favored phase and is the phase obtained after prolonged heating.

Pure silica SSZ-23 can be synthesized using hydroxide or fluoride anions as mineralizers. In the material prepared using F^-, the charge of the SDA is balanced mainly by occluded fluoride and there is only a fairly small concentration of $Si-O^-$ $HO-Si$ couples. About half of these are annealed upon calcination, yielding a silica framework with a high degree of local order, as suggested by the high resolution of $Si(OSi)_4$ resonances in the ^{29}Si MAS NMR spectrum. By contrast, in OH^- medium there is a large concentration of defects of connectivity even after calcination, and the low resolution in the ^{29}Si MAS NMR spectrum suggests a much-decreased local order.

The synchrotron X-ray powder diffraction study produces results that agree with both the ^{29}Si MAS NMR and the computer simulations. The agreement between the results of the Rietveld refinement and the lattice energy minimization studies is especially remarkable, particularly when one considers the complexity of the SSZ-23 structure. The calculated lattice energy for SSZ-23 fits almost exactly on to the expected correlation between lattice energy and framework density that has been reported for a number of other zeolitic structures. This shows that the SSZ-23 structure has comparable stability to other zeolites of similar framework density and that lattice energy is not intrinsically affected by the presence of large odd-membered ring systems.

Acknowledgment. R.E.M. thanks the Royal Society for a University Research Fellowship. I.J.S. thanks the Royal Society of Edinburgh for the provision of a BP Research Fellowship. M.-J.D.-C. and M.A.C. acknowledge financial support by the Spanish CICYT (project MAT97-0723). The authors thank Drs. Andy Fitch and Gavin Vaughan for their help in collecting the synchrotron X-ray data, and the EPSRC and ESRF for financial support.

CM991057R